Low threshold Er^{3+}/Yb^{3+} co-doped microcavity laser

Hsiu-Sheng Hsu[a], Can Cai[b], and Andrea M. Armani[a, c*]

[a]*Mork Family Department of Chemical Engineering and Materials Science, University of Southern California,Los Angeles, California 90089, USA*

[b]*Department of Chemical Engineering, California Institute of Technology, Pasadena, California 91125, USA*

[c]*Ming Hsieh Department of Electrical Engineering-Electrophysics, University of Southern California, Los Angeles, California 90089, USA*

[*] armani@usc.edu

ABSTRACT

An Erbium:Ytterbium codoped microcavity-based laser which is lithographically fabricated from sol-gel is demonstrated. Both single-mode and multimode lasing is observed in the C band (1550nm). The quality factor and pump threshold are experimentally determined for a series of erbium and ytterbium doping concentrations, verifying the inter-dependent relationship between the two dopants. The lasing threshold of the optimized device is 4.2 μW.

Keywords: Microcavity Devices, Rare-earth doped materials

1. INTRODUCTION

In the past decade, significant progress has been made in the general field of low threshold lasers. Ultra-low threshold lasers which operate in the telecommunications band and which can be integrated with other CMOS compatible elements have been developed. These devices have numerous applications in satellite communications [1, 2], biochemical detection [3, 4] and optical computing [5-10]. To optimize both the pump method and the gain medium is important to achieve sub-mW lasing thresholds. While many different materials can be used as the dopant or gain medium, one of the most promising methods of achieving a sub-mW laser is to use rare-earth ions in a co- or tri-dopant configuration, where the lasing of the primary dopant is enhanced by the secondary one, thus improving the efficiency of the overall system [11-17].

To achieve low threshold lasers, initial research revolved around rare-earth doped, ie Ho, Yb, Er, Nd, optical fiber based-lasers [18]. Although these lasers achieved sub-mW thresholds, their performance is ultimately limited by the short interaction time of the pump laser and the efficiency of the gain medium [19]. However, by replacing the optical fiber with an optical resonant cavity, lower threshold powers can be achieved as a result of the high circulating intensities. Specifically, the resonant re-circulation of light enables significantly larger interaction pathlengths and overlap factors, resulting in lower lasing thresholds.

Among different types of resonant cavities, whispering gallery mode optical cavities are ideal for forming microlasers because of their high quality (Q) factors, which defines the interaction time, and small optical mode volumes [20-24]. Most importantly, it is possible to fabricate arrays of high-Q optical cavities directly on a silicon wafer, resulting in an integrated microlaser array. Using a conventional fiber laser is not able to achieve this kind of integrated silicon device. Previous research has investigated fabricating single ion doped toroid microlasers, ie erbium and ytterbium doped microtoroid resonant cavity lasers using either sol-gel techniques or ion implantation [25-27]. However, it is well-known that co-doped lasers have significantly improved performance over single doped devices, because the secondary dopant (sensitizer) can increase the absorption efficiency of the primary dopant [28, 29]. In this work, an ultra-low threshold co-doped microlaser is made by combining the large optical cross section of Er^{3+}:Yb^{3+} co-doped sol-gel and with the high circulating intensities present in ultra-high-Q optical microcavities. In this configuration, erbium is the primary dopant, and ytterbium acts as the sensitizer.

Moreover, the Er^{3+}:Yb^{3+} co-doped material can be pumped around 980nm and lase at 1550nm, which is another benefit to make this co-doped microlaser. This is distinct from a pure single erbium or ytterbium microlaser. Specifically, the

Integrated Optics: Devices, Materials, and Technologies XIV, edited by Jean-Emmanuel Broquin, Christoph M. Greiner,
Proc. of SPIE Vol. 7604, 76040C · © 2010 SPIE · CCC code: 0277-786X/10/$18 · doi: 10.1117/12.848373

pump wavelength for an Yb^{3+} microlaser is 970 nm , with lasing at 1040nm [25]. For an Er^{3+} microlaser, the lasing wavelength is at 1550nm; however, the pump wavelength is at 1480nm [26]. The availability of 980nm pump lasers makes the co-doped microlaser preferred over the Er^{3+} microlaser.

In the present work, the Er^{3+}:Yb^{3+} co-doped sol-gel microlasers are fabricated in arrays on a silicon wafer from co-doped sol-gel using a combination of planar photolithography and CO_2 laser reflow. Several different experimental studies are performed to characterize the microlaser and optimize its performance. The concentrations of both Er^{3+} and Yb^{3+} are systematically varied to verify the inter-dependence of the lasing threshold and Q factor on the co-dopants. As such, both single-mode and multimode Er^{3+}:Yb^{3+} laser based on a microtoroid optical resonator is observed in the C-band (1550 nm). The lasing threshold is 4.2 μW, and we believe this is the lowest threshold yet achieved with a Er^{3+}:Yb^{3+} co-doped laser.

2. EXPERIMENT

2.1 Fabrication of microlaser

The Er^{3+}:Yb^{3+} co-doped sol-gel microlaser is fabricated on a silicon chip progressively with the sol-gel synthesis and the lithography process. The sol-gel technique is unique and desirable because it is cost-effective, flexible, simple and fast [30, 31]. Using the lithography process provides a versatile way to integrate the silicon-based components on a chip.

To synthesize the sol-gel silica thin film for microlaser fabrication, we refer to research in the Chen and Vahala groups [26, 32]. However, this previous sol-gel synthesis protocol was modified to minimize cracking and enable high quality sol-gel silica. Specifically, first tetraethoxysilane (TEOS) was mixed with ethanol to make the sol-gel liquid. The water was then added to hydrolyze the solution with a 2:1 molar ratio of water to TEOS. Hydrochloric acid is introduced as the catalyst to initiate the gelation. Next, ytterbium nitrate and erbium nitrate are added to the solution in the desired Yb^{3+}, Er^{3+} concentration. To produce the Er^{3+}:Yb^{3+} co-doped sol-gel liquid, the entire mixture is stirred with a magnetic stirrer at room temperature for 2 hrs. To form a sol-gel silica thin film, the Er^{3+}:Yb^{3+} co-doped silica sol-gel is spun onto silicon chip and subsequently annealed at 1000°C for 3 hrs.

The annealing temperature is determined by comparing a Fourier transform infrared (FTIR) spectra of thermally grown oxide with that of a pure (undoped) sol-gel silica. Figure 1 shows a series of thin films at different annealing temperatures. The related Si-O-Si absorption bands, which are near 450 cm^{-1}, 800 cm^{-1} and 1100 cm^{-1}, are clearly shown in figure 1 [33, 34]. The corresponding Si-O-Si absorption bands become stronger at higher annealing temperature. It indicates the enhanced densification of the sol-gel silica film after thermal annealing, which is necessary for further device fabrication. After annealing at 1000°C for 3 hrs, the spectra are nearly identical to that of the thermally grown silica, verifying that the sol-gel silica process is optimized. As characterized using both ellipsometry and profilometry, the thickness of the sol-gel silica film is about 1.2 μm after four cycles of spin-coating and thermal annealing.

Following the formation of sol-gel silica thin film, the sol-gel silica microtoroid resonant cavities are fabricated using the process outlined in figure 2[35]. Specifically, first the circular pads of sol-gel silica are lithographically defined using a combination of photolithography and buffered oxide etching. Next the silicon wafer is undercut using XeF_2, an isotropic etchant, forming the sol-gel silica microdisks supported by the silicon pillars. As can be seen in figure 2 (b), the silicon is removed both vertically and laterally to form the microdisks. Last, the microdisks are reflowed using a CO_2 laser, creating the Er^{3+}:Yb^{3+} co-doped microtoroids. The final reflow step enables the ultra-high Q factors [35]. Because the microtoroid is fabricated on a silicon wafer using standard microelectronics technology, it is compatible with standard CMOS processing and integration methods.

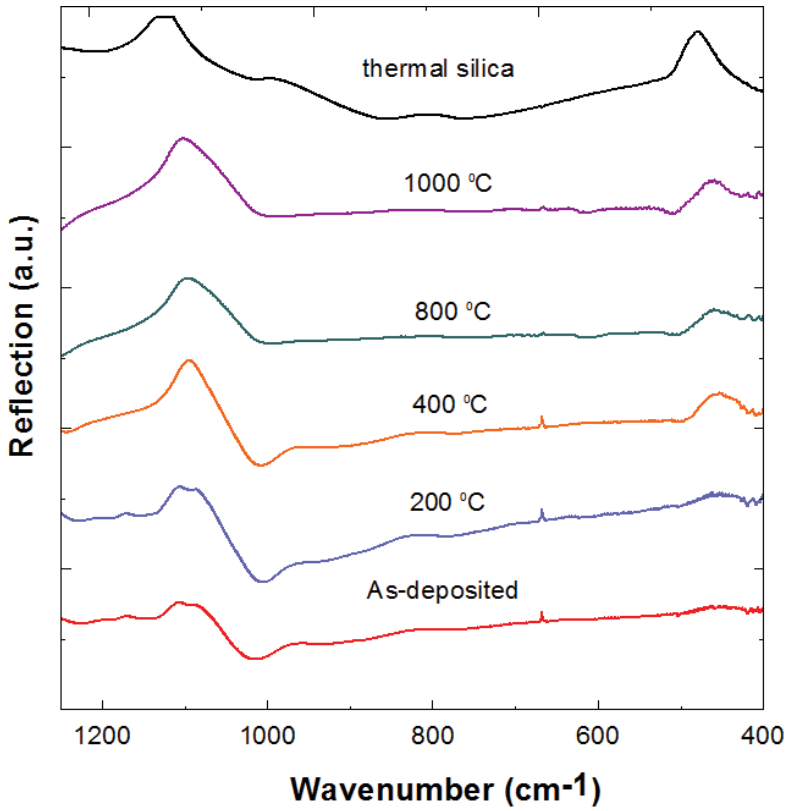

Figure 1. Fourier transform infrared (FTIR) spectra of thermal silica and sol-gel silica thin films prepared at different annealing temperatures. The spectrum of the sol-gel silica annealed at 1000°C is similar to that of the thermally grown silica, indicating that all water has been driven out of the sol-gel matrix.

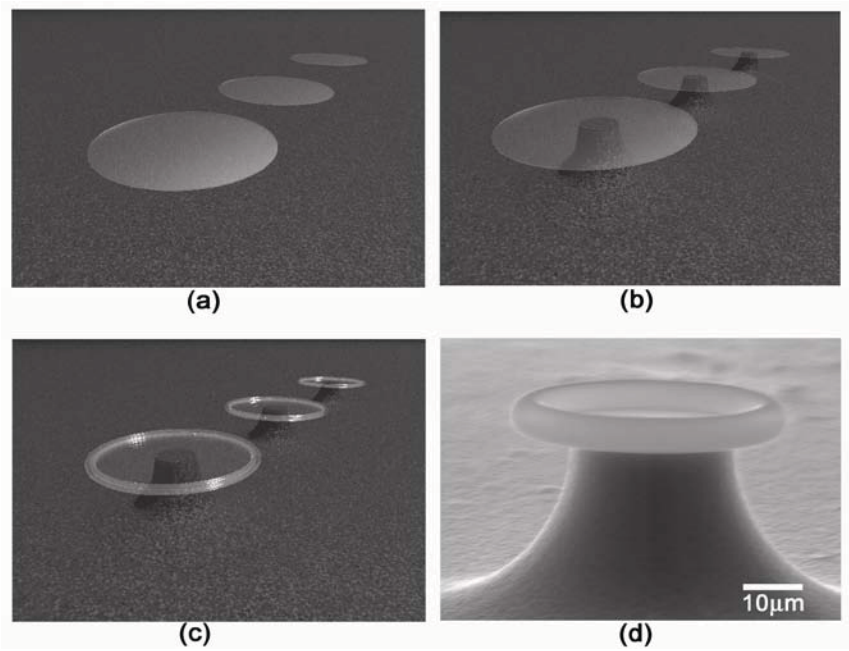

Figure 2. The fabrication process for the sol-gel silica microtoroid resonantors: (a) lithographically patterning and etching circular pads into the sol-gel silica film, (b) undercutting the circular pads with XeF_2 to form the microdisk and (c) reflowing microdisk into microtoroid with the CO_2 laser. (d) A scanning electron-micrograph of the fabricated Er^{3+}:Yb^{3+} co-doped sol-gel microtoroid.

2.2 Experimental set-up

To perform all of the laser and optical device characterization measurements on the co-doped microlaser, a single-frequency, tunable, 980nm CW narrow linewidth (<300 kHz) external cavity laser is used. Tapered optical fiber waveguides are used in the measurements to evanescently couple light in and out of the resonator. Fiber waveguides are fabricated by simultaneously heating the center of a cladding-stripped optical and pulling on both ends. They are a high-efficiency, evanescent method of coupling light to and from the resonant cavities [36, 37]. Tapered fibers for testing at 980/1550 nm were pulled from SMF-28 optical fiber to an average waist diameter of 1μm.

To control the air gap between the taper and the toroid, which determines the cavity lasing performance, the sample is mounted on a three-axis nano-translator for position control. The position of the toroid resonator and the taper is continuously monitored by using a top and side machine vision system. The quality factor is determined by scanning the single-mode laser and measuring the loaded linewidth (full width at half-maximum) in the under-coupled regime. The laser scan frequency is optimized to ensure that neither scan direction (increasing frequency versus decreasing frequency) nor scan frequency has any observable impact on linewidth. The coupling conditions and the position of the resonant frequency are recorded on the computer (NI digitizer, 2GS/s real-time sampling).

An optical spectrum analyzer (OSA) with a resolution of 0.02 nm and a power meter were used to characterize the microlaser performance. A fiber-based 980/1550 nm WDM filter (19 dB isolation) is used to isolate the pump light from the laser emission. The resonant frequency position, linewidth and resonator-taper gap were continuously monitored while the lasing spectra were acquired. In these measurements, coupling into and out of the resonator was approximately 50%. Because a single waveguide is used and the excitation/emission wavelengths are significantly spectrally separated, it is not expected to achieve critical coupling.

3. RESULTS

The optical characteristics of the microresonator device were measured before determining the microlaser performance. For whispering gallery mode resonators, maximizing the Q factor of the device is important because the threshold power is inversely, quadratically related to the Q [26]. In the present set of experiments, the quality factor of the resonant cavity is determined from a linewidth measurement ($Q=\lambda/\delta\lambda$) and is characterized as a function of the Er^{3+}:Yb^{3+} dopant concentration. Therefore, a series of Er^{3+}:Yb^{3+} co-doped sol-gel films are made with different doping concentrations of erbium and ytterbium ions and the Q factors of the resulting devices are measured. It has previously been shown that high quality factors and low doping concentrations are required for a low threshold microlaser [25-27]. However, in these previous systems, there was only one dopant, making this optimization process significantly more straightforward.

Figure 3 shows the measured quality factors as function of the two dopants with different concentrations. As expected from classic resonator physics, the quality factor is dominated by doping concentrations because of the influence of the dopants on cavity loss [25, 27]. Specifically, the addition of Yb^{3+}, which is on-resonance at 980nm, has a much stronger impact on the cavity Q than does the addition of Er^{3+}, which is off-resonance at 980nm. It is noted that Q factors as high as $1.3\text{x}10^7$ were measured at 980nm in the undoped sol-gel silica microtoroids, further verifying the sol-gel purity. Additionally, all Q factor measurements were performed at 980nm or the pump wavelength of the microlaser. It is expected that the Q factor will be different at the lasing wavelength.

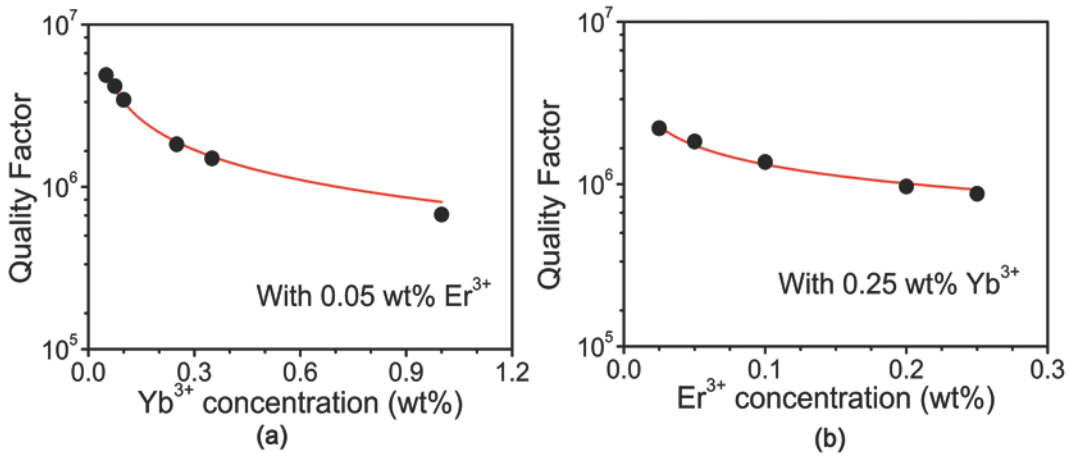

Figure 3. Measured Q factors (performed at pump wavelength of 980 nm) as a function of erbium/ytterbium concentrations. (a) Operation of microtoroid with erbium concentration ranging from 0.025 to 0.25wt%, with the ytterbium concentration fixed at 0.25 wt%. (b) Operation of microtoroid with ytterbium concentration ranging from 0.05 to 1wt%, with the erbium concentration fixed at 0.05 wt%.

As described experimental set-up, a single fiber taper is used to couple light into and out of the microtoroid cavities as shown in figure 4 (a). The lasing is coupled back into the same optical fiber used for excitation, enabling direct measurement on an optical spectrum analyzer (OSA). The single-mode or multi-mode lasing action can be observed between 1520 to 1570nm. Figure 4 (b) shows a typical single-mode lasing spectrum of Er^{3+}:Yb^{3+} co-doped microtoroid laser. The ability to easily achieve ultra low threshold, single mode lasing is a result of the relatively few higher-order, high Q optical modes present in microtoroid optical cavities. This ability is one of the advantages of using a planar geometry such as a microtoroid or microring resonator which inherently suppresses the azimuthal modes of the cavity which can act as parasitic loss in microsphere resonant cavities [26]. Additionally, the mode volume of a microtoroid is smaller than that of a microsphere [38]. Figure 3(c) shows the emission spectrum of a Er^{3+}:Yb^{3+} co-doped microtoroid laser with a 40μm diameter. The spacing between the lasing lines corresponds with the free-spectral range (FSR) of the microtoroid resonator, which is approximately 13nm and is in good agreement with the theoretically predicted value. Therefore, using a single platform, it is possible to controllably adjust between single and multi-mode lasing.

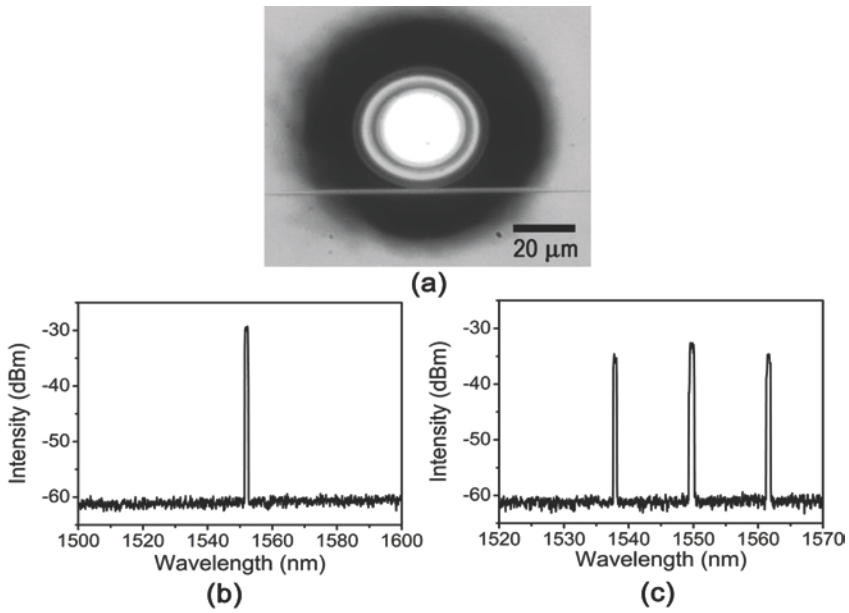

Figure 4. (a) A top-view optical photograph of the testing setup of a Er^{3+}:Yb^{3+} co-doped microtoroid laser coupled by a fiber taper. (b) Typical emission spectrum of a single-mode Er^{3+}:Yb^{3+} co-doped microtoroid laser. (b) Typical emission spectrum of a multi-mode Er^{3+}:Yb^{3+} co-doped microtoroid laser.

Figure 4 shows a single-mode microlaser with the lasing threshold of of 4.2μW. Above threshold, the laser output power increases linearly with the absorbed pump power as shown in figure 5. This ultralow threshold is a result of the high quality factor of the device, small mode volume of the microtoroid, and homogeneous distribution of the co-dopants inside the toroid, which enables the optimized overlap between the pump modes and active region [26]. It is important to note that while recent Er^{3+}:Yb^{3+} co-doped lasers based on microsphere resonant cavities have demonstrated thresholds of 30μW to 50μW [39, 40], a lithographically fabricated co-doped Er^{3+}:Yb^{3+} microlaser has never been demonstrated to the author's knowledge.

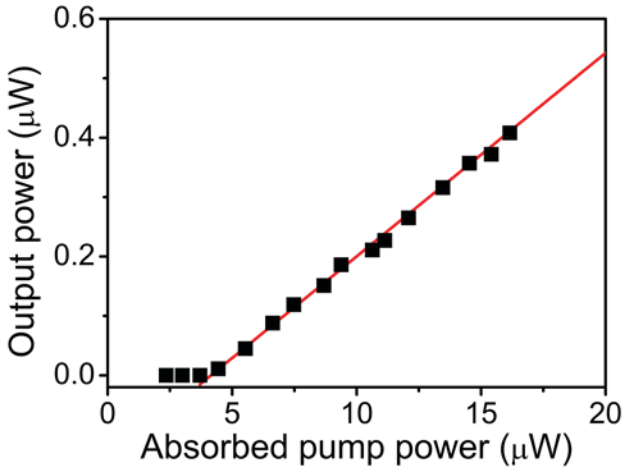

Figure 5. Measured laser output power versus the absorbed pump power for an Er^{3+}:Yb^{3+} co-doped microlaser with principal diameter of 40 μm.

The threshold was determined for a series of different doping concentrations of erbium and ytterbium ions. Generally, low doping concentrations result in a low threshold power. By varying the doping concentration of erbium and ytterbium ions independently, we verified this effect in the present co-dopant system, by determining the threshold at each concentration.

Figure 6 demonstrates the lasing threshold as a function of the two dopants with different concentrations. The minimum threshold is at an erbium concentration of 0.05 wt% and ytterbium concentration of 0.075 wt% as shown in figure 6. For erbium concentrations greater than 0.05 wt%, the threshold power increases from concentration dependent loss mechanism, such as ion-pair induced quenching. The threshold increases again at low concentrations because erbium ions are not able to give sufficient gain for loss compensation. Similarly, above 0.075 wt% concentration of ytterbium ions, the pump threshold increases because it needs the additional pump power to compensate for the loss from unpumped ytterbium ions. Below 0.075 wt% concentration of ytterbium ions, the lasing threshold raises because the doping ytterbium concentration is not high enough to overcome the intrinsic loss of the cavity and to transfer energy from Yb^{3+} to Er^{3+} efficiently.

It should be noted that other commonly seen effects in co-doped lasers, such as the upconversion of Er^{3+} and simultaneous lasing at both 1040nm and 1550nm resulting from both Yb^{3+} and Er^{3+} excitation, were also seen at different Er^{3+}:Yb^{3+} concentration ratios. Comparing these results with the cavity Q factors, the mechanism of lasing action in co-doped systems is more complex than in single dopant systems. It is a result of the different emission and absorption cross sections of two dopants, the spatial selectivity of the pump, and the method of energy transfer.

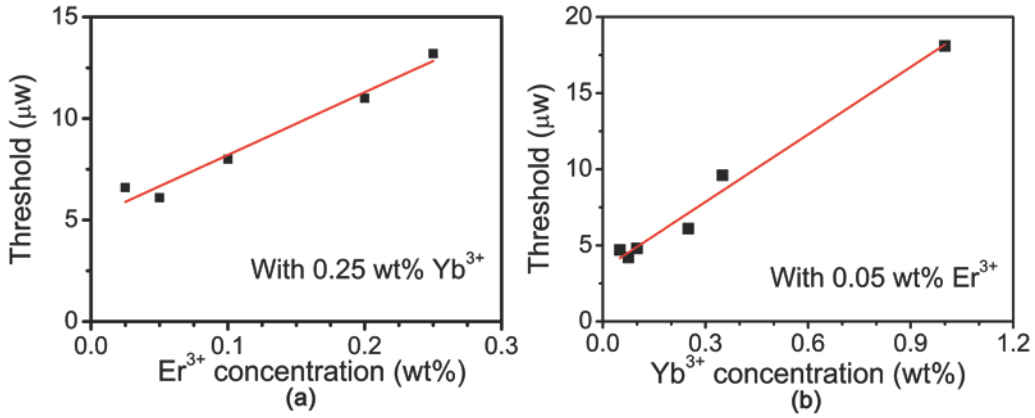

Fig. 6. Microlaser threshold plotted as a function of co-dopant concentration. The threshold was determined for a series of different doping concentrations of erbium and ytterbium ions. (a) Varying Er^{3+} concentration with 0.25 wt% Yb^{3+} concentration. (b) Varying Yb^{3+} concentration with 0.05 wt% Er^{3+} concentration. The minimum threshold achieved is 4.2μW at Er^{3+} concentration of 0.05 wt% and Yb^{3+} concentration of 0.075 wt%.

4. CONCLUSION

In the present work, we have fabricated an ultralow threshold Er^{3+}:Yb^{3+} co-doped toroidal microlaser on a silicon chip. We developed a sol-gel synthesis process which formed a uniform host matrix for the co-dopants of erbium and ytterbium ions to enable lithographic fabrication of these co-doped devices.

By adjusting the coupling conditions, we have demonstrated single-mode and multi-mode lasing action between 1520 and 1570 nm. The quality factor and pump threshold have been verified to depend strongly on both the doping concentration and the specific dopant.

The lasing threshold is as low as 4.2μW, which is more than seven times lower than the previously reported lowest threshold to date for a Er^{3+}:Yb^{3+} co-doped laser, which was based on a microsphere resonant cavity [39]. Ultra-low threshold on-chip microlasers are easily integrated with other silicon-based components, paving the way for improved signal processing [5-10], biochemical detection [3, 4] and free-space communication [1, 2].

ACKOWLEDGEMENTS

The authors would like to thank Prof. Mark Thompson at the University of Southern California for aid in the sol-gel preparation. This work was supported by the National Science Foundation [0852581], and the Army Research Lab [W911NF-09-0041]. H. Hsu was supported by an Alfred Mann Institute Graduate Research Fellowship. C. Cai was supported by a William Lacey Summer Undergraduate Research Fellowship. Additional information can be found at http://armani.usc.edu

REFERENCES

[1] Y. Jeong, *et al.*, "A 43-W C-band tunable narrow-linewidth erbium-ytterbium codoped large-core fiber laser," *Ieee Photonics Technology Letters,* vol. 16, pp. 756-758, Mar 2004.

[2] M. Guelman, *et al.*, "Acquisition and pointing control for inter-satellite laser communications," *IEEE Transactions on Aerospace and Electronic Systems,* vol. 40, pp. 1239-1248, Oct 2004.

[3] C. Monat, *et al.*, "Integrated optofluidics: A new river of light," *Nature Photonics,* vol. 1, pp. 106-114, 2007.

[4] J. Yang and L. J. Guo, "Optical sensors based on active microcavities," *IEEE Journal of Selected Topics in Quantum Electronics,* vol. 12, pp. 143-147, Jan-Feb 2006.
[5] M. Ferrera*, et al.*, "Low-power continuous-wave nonlinear optics in doped silica glass integrated waveguide structures," *Nature Photonics,* vol. 2, pp. 737-740, 2008.
[6] G. T. Reed, "Device physics - The optical age of silicon," *Nature,* vol. 427, pp. 595-596, 2004.
[7] P. Thilakan*, et al.*, "Fabrication and characterization of a high Q microdisc laser using InAs quantum dot active regions," *Nanotechnology,* vol. 18, 2007.
[8] H. S. Rong*, et al.*, "Low-threshold continuous-wave Raman silicon laser," *Nature Photonics,* vol. 1, pp. 232-237, 2007.
[9] J. Cousin*, et al.*, "Application of a continuous-wave tunable erbium-doped fiber laser to molecular spectroscopy in the near infrared," *Applied Physics B-Lasers and Optics,* vol. 83, pp. 261-266, 2006.
[10] P. Laporta*, et al.*, "Frequency locking of tunable Er:Yb microlasers to absorption lines of (C2H2)-C-13 in the 1540-1550 nm wavelength interval," *Applied Physics Letters,* vol. 71, pp. 2731-2733, Nov 1997.
[11] D. Milanese*, et al.*, "Investigation of infrared emission and lifetime in Tm-doped 75TeO(2): 20ZnO : 5Na(2)O (mol%) glasses: Effect of Ho and Yb co-doping," *Journal of Non-Crystalline Solids,* vol. 354, pp. 1955-1961, 2008.
[12] I. K. Battisha, "Visible up-conversion photoluminescence from IR diode-pumped SiO2-TiO2 nano-composite films heavily doped with Er3+-Yb3+ and Nd3+-Yb3+," *Journal of Non-Crystalline Solids,* vol. 353, pp. 1748-1754, 2007.
[13] Y. J. Chen*, et al.*, "1.1 W diode-pumped Er : Yb laser at 1520 nm," *Optics Letters,* vol. 32, pp. 2759-2761, 2007.
[14] S. F. Li*, et al.*, "Absorption and photoluminescence properties of Er-doped and Er/Yb codoped soda-silicate laser glasses," *Journal of Applied Physics,* vol. 96, pp. 4746-4750, Nov 2004.
[15] A. F. Obaton*, et al.*, "Yb3+-Er3+-codoped LaLiP4O12 glass: a new eye-safe laser at 1535 nm," *Journal of Alloys and Compounds,* vol. 300, pp. 123-130, 2000.
[16] J. T. Kringlebotn*, et al.*, "HIGHLY-EFFICIENT, LOW-NOISE GRATING-FEEDBACK ER3+YB3+ CODOPED FIBER LASER," *Electronics Letters,* vol. 30, pp. 972-973, Jun 1994.
[17] C. Li*, et al.*, "ROOM-TEMPERATURE CW LASER ACTION OF Y2SIO5-YB-3+,ER-3+ AT 1.57-MU," *Optics Communications,* vol. 107, pp. 61-64, 1994.
[18] P. Urquhart, "Review of rare earth doped fibre lasers and amplifiers," *Optoelectronics, IEE Proceedings J,* vol. 135, pp. 385-407, 1988.
[19] M. J. F. Digonnet, *Rare-earth-doped fiber lasers and amplifiers*, 2nd ed. New York: Marcel Dekker, 2001.
[20] K. Srinivasan*, et al.*, "Cavity Q, mode volume, and lasing threshold in small diameter AlGaAs microdisks with embedded quantum dots," *Optics Express,* vol. 14, pp. 1094-1105, Feb 2006.
[21] F. Lissillour*, et al.*, "Whispering-gallery-mode laser at 1.56 mu m excited by a fiber taper," *Optics Letters,* vol. 26, pp. 1051-1053, Jul 2001.
[22] M. L. Gorodetsky*, et al.*, "Ultimate Q of optical microsphere resonators," *Optics Letters,* vol. 21, pp. 453-455, Apr 1 1996.
[23] V. Sandoghdar*, et al.*, "Very low threshold whispering-gallery-mode microsphere laser," *PHYSICAL REVIEW A,* vol. 54, 1996.
[24] S. X. Qian*, et al.*, "LASING DROPLETS - HIGHLIGHTING THE LIQUID-AIR INTERFACE BY LASER-EMISSION," *Science,* vol. 231, pp. 486-488, 1986.
[25] E. P. Ostby*, et al.*, "Ultralow-threshold Yb3+: SiO2 glass laser fabricated by the solgel process," *Optics Letters,* vol. 32, pp. 2650-2652, Sep 15 2007.
[26] L. Yang*, et al.*, "Erbium-doped and Raman microlasers on a silicon chip fabricated by the sol-gel process," *Applied Physics Letters,* vol. 86, p. 3, Feb 2005.
[27] B. Min*, et al.*, "Erbium-implanted high-Q silica toroidal microcavity laser on a silicon chip," *Physical Review A,* vol. 70, 2004.

[28] L. D. da Vila, *et al.*, "Mechanism of the Yb-Er energy transfer in fluorozirconate glass," *Journal of Applied Physics,* vol. 93, pp. 3873-3880, 2003.
[29] P. Laporta, *et al.*, "Erbium-ytterbium microlasers: optical properties and lasing characteristics," *Optical Materials,* vol. 11, pp. 269-288, 1999.
[30] G. Kakarantzas, *et al.*, "Low-loss deposition of solgel-derived silica films on tapered fibers," *Optics Letters,* vol. 29, pp. 694-696, Apr 2004.
[31] A. Selvarajan and T. Srinivas, "Optical amplification and photosensitivity in sol-gel based waveguides," *IEEE Journal of Quantum Electronics,* vol. 37, pp. 1117-1126, 2001.
[32] L. L. Yang, *et al.*, "Compositional tailored sol-gel SiO2-TiO2 thin films: Crystallization, chemical bonding configuration, and optical properties," *Journal of Materials Research,* vol. 20, pp. 3141-3149, 2005.
[33] P. Innocenzi, *et al.*, "Structure and Properties of Sol-Gel Coatings from Methyltriethoxysilane and Tetraethoxysilane," *Journal of Sol-Gel Science and Technology,* vol. 3, pp. 47-55.
[34] L. L. Yang, *et al.*, "Compositional tailored sol-gel SiO2-TiO2 thin films: Crystallization, chemical bonding configuration, and optical properties (vol 20, pg 3141, 2005)," *Journal of Materials Research,* vol. 21, pp. 802-802, Mar 2006.
[35] D. K. Armani, *et al.*, "Ultra-high-Q toroid microcavity on a chip," *Nature,* vol. 421, pp. 925-928, Feb 2003.
[36] D. W. Vernooy, *et al.*, "High-Q measurements of fused-silica microspheres in the near infrared," *Optics Letters,* vol. 23, pp. 247-249, Feb 15 1998.
[37] M. Cai and K. Vahala, "Highly efficient hybrid fiber taper coupled microsphere laser," *Optics Letters,* vol. 26, pp. 884-886, 2001.
[38] K. J. Vahala, "Optical microcavities," *Nature,* vol. 424, pp. 839-846, 2003.
[39] C. H. Dong, *et al.*, "Low-threshold microlaser in Er : Yb phosphate glass coated microsphere," *Ieee Photonics Technology Letters,* vol. 20, pp. 342-344, Mar-Apr 2008.
[40] Y. F. Xiao, *et al.*, "Low-threshold microlaser in a high-Q asymmetrical microcavity," *Optics Letters,* vol. 34, pp. 509-511, 2009.